



Analysis of dynamic displacement of reinforced concrete deep beams made of high strength concrete

Part I: Analysis of dynamic displacement of a reinforced concrete deep beam made of high strength C100 grade concrete

WALDEMAR CICHORSKI

Military University of Technology, Faculty of Civil Engineering and Geodesy,
2 Gen. W. Urbanowicza Str., 00-908 Warsaw, Poland, waldemar.cichorski@wat.edu.pl

Abstract. The work presented is a three-part set of studies containing a comparative analysis of the displacement state of rectangular concrete deep beams made of concrete of different classes of very high strength, loaded dynamically. The analysis was carried out on the basis of the method presented in this paper [1], which allows for the physical nonlinearity of structural materials: concrete and reinforcing steel to be taken into account. Each part of the work contains the results of numerical solutions of the displacement state of the deep beams separately for the concrete strength of *C100* grade, *C200* grade, and *C300* grade, in each case reinforced with ordinary steel and increased strength steel. Comparative analysis is carried out in Part Two and Part Three, where the results obtained in these parts are respectively compared with the results obtained in the preceding parts. The analysis includes the mutual relations of mechanisms for achieving dynamic load carrying — capacity. The results describing the variation of displacements in time indicate the characteristic features of the deep beam effort and allow for the inference on reaching the state of the dynamic load carrying — capacity. In general, the work confirmed the accuracy of the assumptions and deformation models of concrete and steel as well as the effectiveness of methods of analysis proposed in paper [1] for the problems of numerical simulation of reinforced concrete deep beams behaviour under dynamic loading.

The key assumptions used in the analysis are presented in the first part of the paper. The characteristic features of structural materials: concrete and reinforcing steel are presented, taking into account the modified idea of modelling of the dynamic properties of concrete as a material of very high strength. An analysis of the displacement state of rectangular reinforced concrete deep beams made of very high strength concrete of *C100* grade under dynamic load for two types of reinforcing steel — ordinary and increased strength — was carried out.

Key words: mechanics of structures, reinforced concrete structures, deep beams, dynamic load, physical nonlinearity

DOI: 10.5604/01.3001.0011.8056

1. Introduction

1.1. Characteristics of the work

The aim of the work is the analysis of the influence of the very high strength of concrete on displacement (deformation) of rectangular reinforced concrete deep beams loaded dynamically with the inclusion of physical nonlinearity of construction materials: concrete and steel. The solution was acquired with the use of the method of analysis of non-elastic behaviour of the reinforced dynamically loaded concrete deep beam [1].

The essence of this method consists in the following elements: dynamic modelling of the material properties, modelling of the process of deformation of the flat construction framework — a reinforced concrete deep beam, and also algorithmisation and numeric programming of the solution. Modelling of the properties of construction materials was carried out with the use of the assumptions of flow plasticity theory. The model of plastic/ideally viscoplastic material was used for reinforced steel, taking into account the plastic retardation effect. Modelling the dynamic properties of concrete was the topic of the considerations of many publications, i.a. [10, 11]. As far as concrete is concerned, the work adopted a non-standard model of the dynamic deformation of concrete [2]. This model describes the elastic properties of concrete, the limited properties of ideal viscoplasticity on the initial dynamic surface of plasticity, material softening and volume changes. The degradation of the deformation module was ignored in the model. The adopted concrete model facilitates a simplified description of material cracking or crushing as states of loss of load capacity achieved in the process of material weakening. Achieving the goal required introduction of constant properties into the adopted concrete model, allowing the description of the properties of concrete of very high strength. An assumption was adopted, in the modified concrete model, that the boundary deformation values may be variable and dependent on the class of concrete [3, 4]. The analysis method of the effort of the construction form was formulated with the use of the principles of the finite element method [5]. For the reinforced concrete deep beam, treated as a composite material consisting of the concrete matrix strengthened with thin bars of steel reinforcing, a hypothesis for the cooperation of the reinforcing rods and matrix material was proposed. The solution of dynamic systems of the displacement equations for the displacement of the finite element method was conducted on the basis of algorithms and programmes of numerical analysis of the flat tension state, which allows for the identification of the states of displacement, deformation, and deformation and tension speed with the inclusion of the effects of physical material nonlinearity, including concrete scratching.

The work presented the results of numerical solutions for the reinforced concrete deep beam, which was the topic of static experimental research of F. Loenhardt and

R. Walter, [6]. The work also included an analysis of the deformation of the reinforced concrete deep beam made of *C100*, *C200* and *C300* high-strength concrete, and reinforced with regular and increased strength steel. A variability was indicated in the time of the basic displacement parameter — vertical displacement of selected points of the deep beam, and an analysis was carried out regarding the influence of the very high strength concrete and increased strength steel on displacement of concrete deep beams, taking into account the nonlinearity of physical construction materials. The interrelations of the mechanism of achieving dynamic carrying capacity as the limit load level, at which the deep beam does not display signs of instability displacement behaviour, were assessed under the analysis.

The work was divided into three parts. Part One presents the main assumptions established under the analysis and the results of the analyses for the reinforced concrete deep beam made of *C100* concrete and reinforced with regular and increased strength steel. Part Two presents the results of the analysis of dynamic deformation of the concrete deep beam made of *C200* concrete reinforced with regular and increased strength steel with a comparative analysis of the results in relation to the deep beam made of *C200* concrete. Finally, Part Three presents the results of the analyses for the concrete deep beam made of *C300* concrete reinforced, just as the previous deep beams, with regular and increased strength steel with a comparative analysis and assessment of the results in relation to the deep beam made of *C100* and *C200* concrete.

1.2. Subject of the analysis

The subjects of the analysis are deep beams made of concrete matrix strengthened with thin, steel reinforcement bars in orthogonal arrangement. The deep beam is subjected to load on the upper edge, constant over time, with equally distributed dynamic load $p(x, t) = p = \text{const}$. Load was assumed to be of impulse type i.e. suddenly applied in the moment $t = 0$. For the purpose of stability verification of the calculation method, it was additionally assumed that the impulse load will be constantly applied to the upper edge of the structure — as a result it was established $p(x, t) = p = \text{const}$.

A numerical analysis was applied to a rectangular reinforced concrete deep beam with orthogonally arranged reinforcement, designated in the paper of F. Leonhardt and R. Walther [6] as WT3, fig. 1. The deep beam was the subject of the analysis in paper [7].

The dimensions of the deep beam are: length, height: $L = B = 160$ cm, thickness: $t = 10$ cm. The main reinforcement of the deep beam was made in the form of 4 layers of reinforcement loops of *A-III* with a yield point of $f_y = 410$ MPa, the diameter of the bars of f_8 , placed in the lower part of the deep beam. The remaining part of the deep beam is reinforced with vertical and horizontal stirrup reinforcement made of steel with a yield point of $f_y = 240$ MPa, the diameter of the bars of f_5 , and

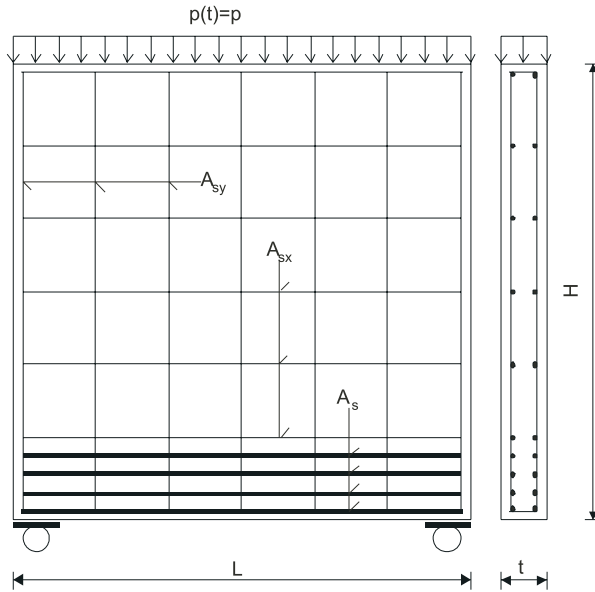


Fig. 1. A diagram of reinforced concrete deep beam

spacing of 26 cm. The concrete matrix was made of concrete with the a compressive strength of $f_c = 30$ MPa and tensile strength of $f_t = 3$ MPa.

Taking into account the use in the numerical construction analysis of high strength concrete, paper [8] included a proposed modification of the concrete deformation model. The essence of the proposed modification of the concrete model is the change in the interpretation of the size of boundary deformation ε_{fc} for the phase of ideal viscoplasticity and ε_{uc} for the phase of material weakening. In the basic version of the model, on the basis of the analysis of the results of experimental research, boundary deformations ε_{fc} are determined as constant values for single-axis compression of 2‰, regardless of the concrete class, whereas for boundary deformations ε_{uc} the values were determined within the range of $\varepsilon_{uc} = (6-12)\%$, on condition that lower values ε_{uc} may be used for concrete of a higher class, and higher values ε_{uc} for concrete of lower and medium class, but without exact designation of the relation with the concrete class. Currently, in the modified concrete deformation model, it is assumed that the boundary deformation values ε_{fc} and ε_{uc} may be variable and dependent on the concrete class, in accordance with the concrete strength variability function specifying so-called strength indicator, as described in paper [8].

As a consequence, material properties describing the constitutive concrete model, shown in table 1, were adopted for the numerical analysis.

TABLE 1

Limit parameter values describing the concrete model

Concrete Class	f_c [MPa]	f_t [MPa]	e_{ec} [‰]	e_{fc} [‰]	e_{uc} [‰]	E_c [GPa]
C30	30	3	1.20	2.00	12.00	25.0
C100	100	10	2.08	2.80	11.25	48.0
C200	200	20	3.88	4.49	10.71	51.50
C300	300	30	5.71	6.21	10.21	52.5

Graphic interpretation of material parameters describing the constitutive concrete model shown in fig. 2, in the plane of stresses and deformation for single-axis compression. In this picture, the indicator Ψ_d describes the dynamic strength of concrete in accordance with the model described in the paper [2].

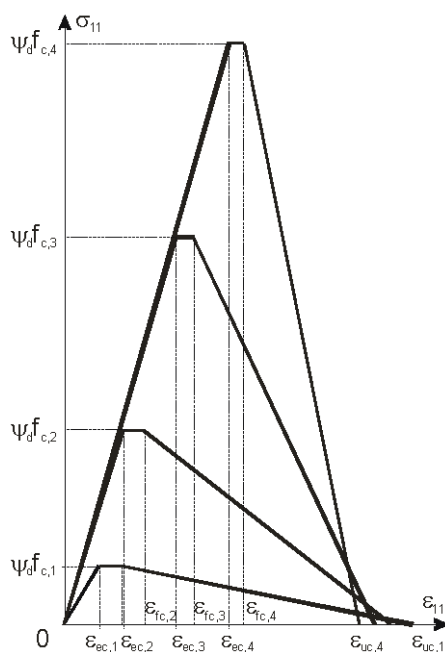


Fig. 2. Graphic interpretation of the material parameters of the constitutive concrete model

For increased strength steel a modification was made to the steel strength parameters of the main reinforcement of the deep beam, i.e. rods with the diameter of f8. Modification involved using steel class A-H with a yield point of $f_y = 690$ MPa.

The intensity of dynamic load designates the dimensionless parameter $\alpha = P/P_0$ of an auxiliary, total load of the deep beam $P_0 = p \times L$, in relation to the level of static

deep beam carrying capacity P_0 . The assessment of the level of static deep beam carrying capacity in relation to each deep beam type, in accordance with [9], amounts to:

- for *C100*, *C200*, *C300* concrete and *A-III* steel:

$$P_0 = [2210 \text{ kN} / 2595 \text{ kN} / 3317 \text{ kN}],$$

- for *C100*, *C200*, *C300* concrete and *A-H* steel:

$$P_0 = [2085 \text{ kN} / 3028 \text{ kN} / 3999 \text{ kN}].$$

Part One presents the main assumptions established under the analysis carried out. The characteristic features of structural materials: concrete and reinforcing steel are presented, taking into account the modified idea of modelling of dynamic properties of concrete as a material of very high strength. A deformation analysis (displacement state) of rectangular reinforced concrete deep beams made of concrete of very high strength loaded dynamically was carried out — in this part of the work the considerations were limited to the analysis of the deformation of the deep beam made of *C100* grade concrete reinforced with regular and increased strength steel. A variability was indicated in the time of the basic displacement parameter — vertical displacement of selected points of the deep beam, and an analysis was carried out regarding the influence of the very high strength concrete and increased strength steel on displacement of concrete deep beams, taking into account the nonlinearity of physical construction materials.

2. Analysis of numerical results

In order to illustrate the influence of concrete of very high strength and increased strength steel on the deformation of rectangular reinforced concrete deep beams, numerical experiments were carried out for the deep beam of reinforcement arranged as in experiment [6] and with modified parameters describing the constitutive concrete model (concrete class *C100*). Additionally, the influence of changing the strength parameters of reinforcing steel, i.e. the influence of replacement *A-III* ordinary steel, similarly to experiment [6], for steel of increased strength (*A-H*), was analysed.

For that purpose, the following points in the central section (designated in fig. 3) were adopted for the observation of dynamic changes of displacement of the deep beam: x_d — on the lower edge, x_s — in the centre of the deep beam height, x_g — on the upper edge. In turn, the following points were selected for observation in order to illustrate the variability over time of the lower and upper edge of the deep beam:

- on the lower edge of the deep beam: $x_2, x_4, x_6, x_8, x_{10}, x_{12}, x_{14}, x_{16}, x_{18}$,
- on the upper edge of the deep beam: $x_{290}, x_{292}, x_{294}, x_{296}, x_{298}, x_{300}, x_{302}, x_{304}, x_{306}$,

the designation of which was show in fig. 3.

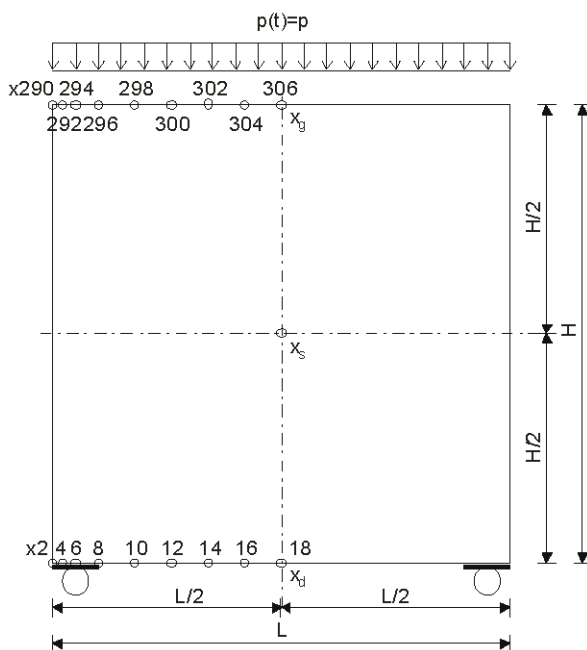


Fig. 3. Designation of points chosen for displacement observation

2.1. Reinforced-concrete deep beam reinforced with ordinary steel (A-III)

Fig. 4 shows the variability of vertical displacement over time of chosen points in the central section for various load levels $\alpha = P/P_0$. For load level $\alpha = 0.3$, fig. 4₁, and fig. 4₂, in the elastic range and with a minor level of plastic processes in concrete, the results indicate, known from elastic solutions, a relation between vertical displacements: $v(x_g) > v(x_s) > v(x_d)$. As the load increases to level $\alpha = 0.4$, fig. 4₃, a significant increase of vertical displacements of the lower point x_d is observed. Because of scratching of the concrete in the lower layers of the shear zone, a partial modification of interrelations occurred before the change over time of each vertical displacement: $v(x_g) > v(x_d) > v(x_s)$. Upon further application of load to the level $\alpha = 0.5$, fig. 4₄, a propagation of scratched areas occurred in the shear zone (in two directions, upwards and diagonally towards the direction of the centre of the span) and in the span area, which caused another modification of interrelations between the change over time of each vertical displacement: $v(x_s) > v(x_d) > v(x_g)$, which applies at intervals of reaching maximum amplitude of displacements. On the level of load $\alpha = 0.6$, fig. 4₅, a lack of stabilisation of plastic processes can be observed, which manifested itself at lower levels of load stabilised by a vibrating movement around permanent displacements of observed points. Only during the initial phase

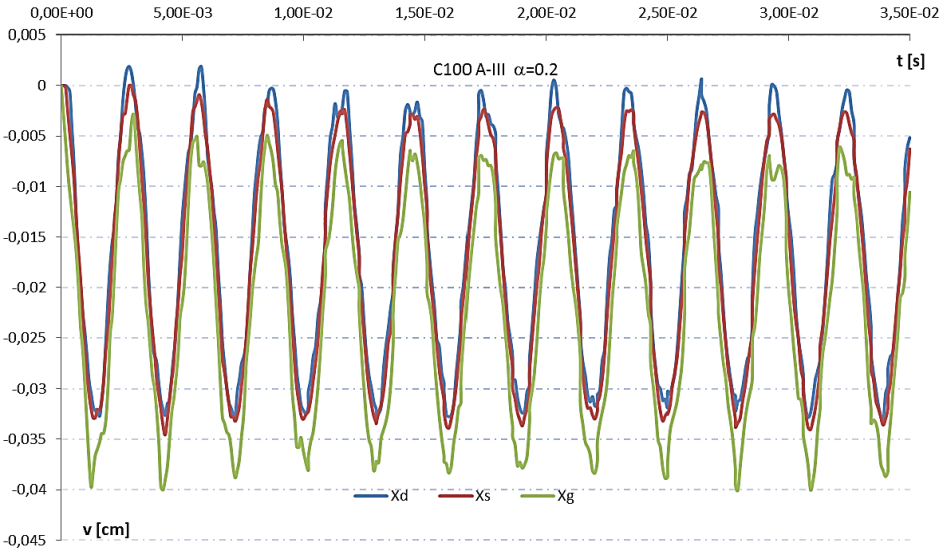


Fig. 4₁. Change over time of vertical displacements of points in the central section for load level $\alpha = 0.2$

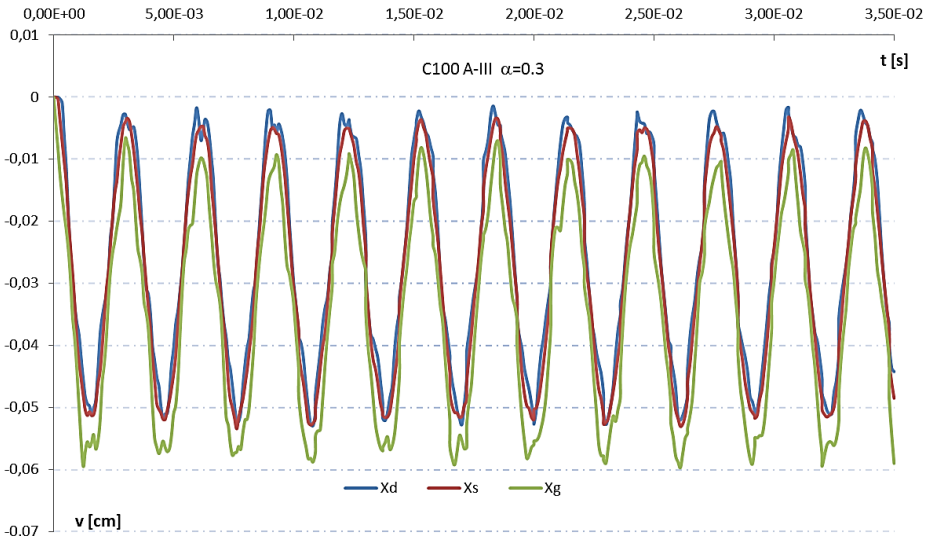


Fig. 4₂. Change over time of vertical displacements of points in the central section for load level $\alpha = 0.3$

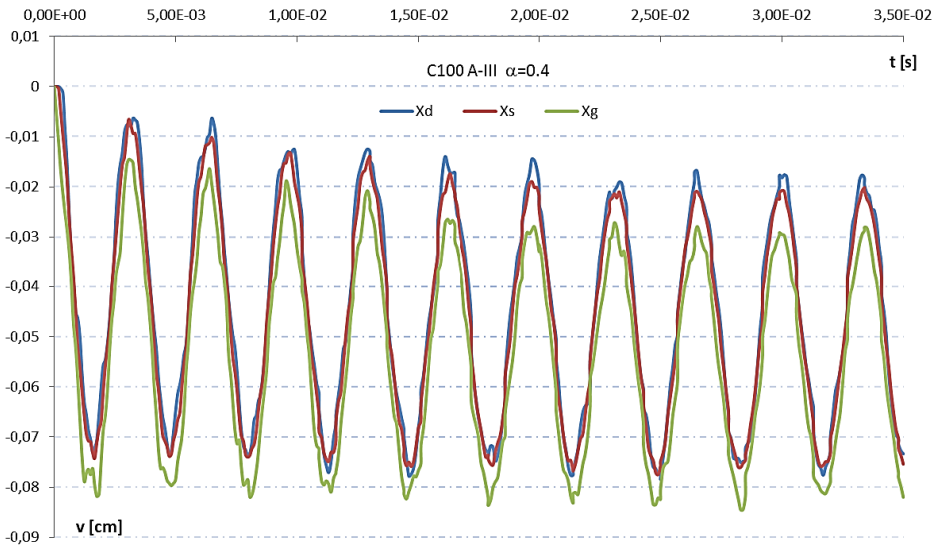


Fig. 4.3. Change over time of vertical displacements of points in the central section for load level $\alpha = 0.4$

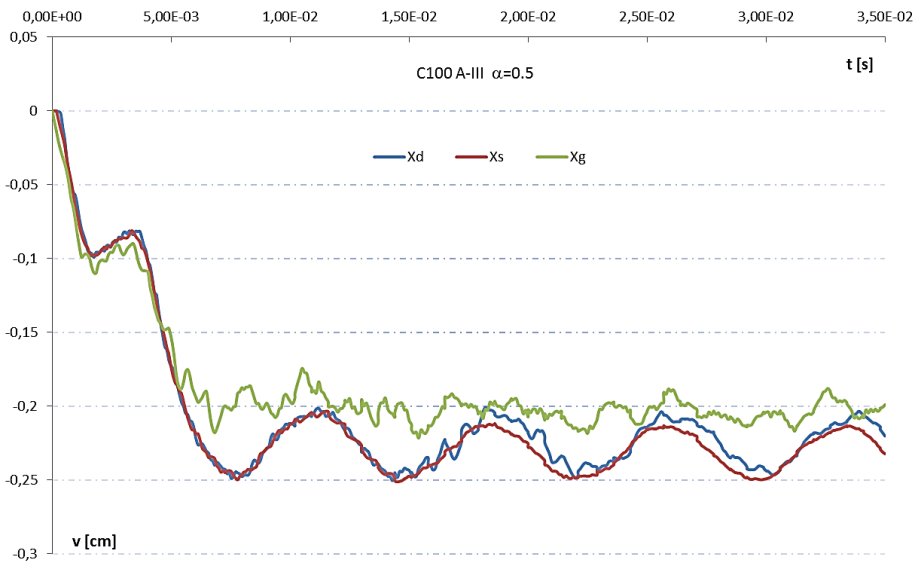


Fig. 4.4. Change over time of vertical displacements of points in the central section for load level $\alpha = 0.5$

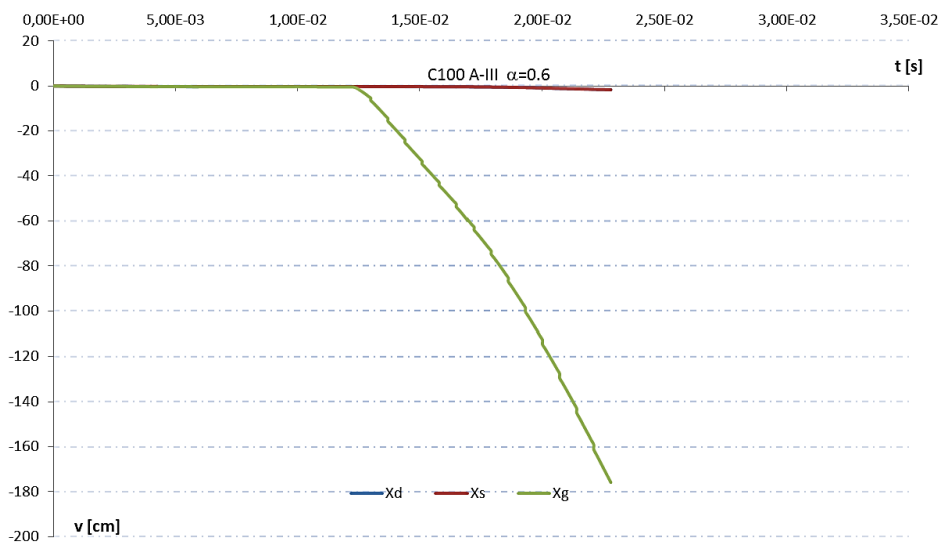


Fig. 4₅. Change over time of vertical displacements of points in the central section for load level $\alpha = 0.6$

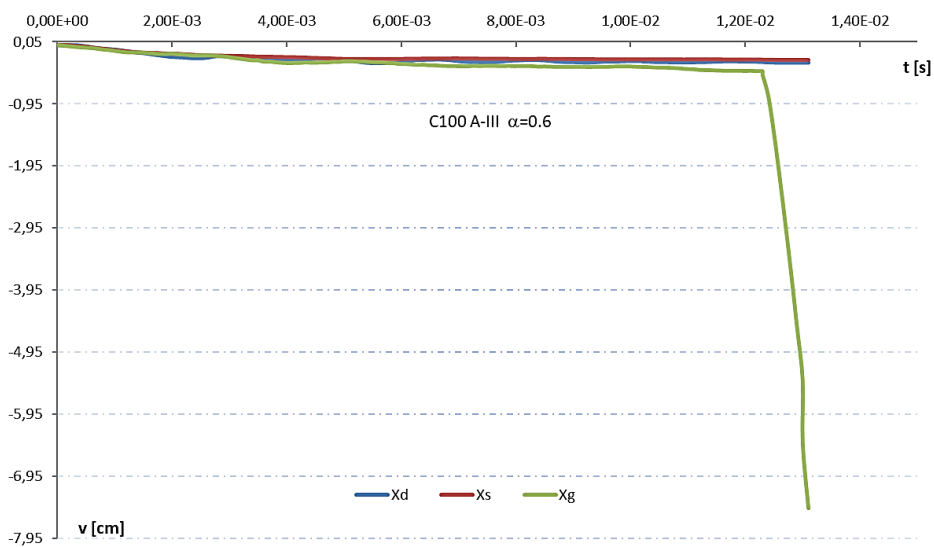


Fig. 4_{5a}. Change over time of vertical displacements of points in the central section for the load level $\alpha = 0.6$ — detail fig. 4₅ (with a reduced time interval of the analysis)

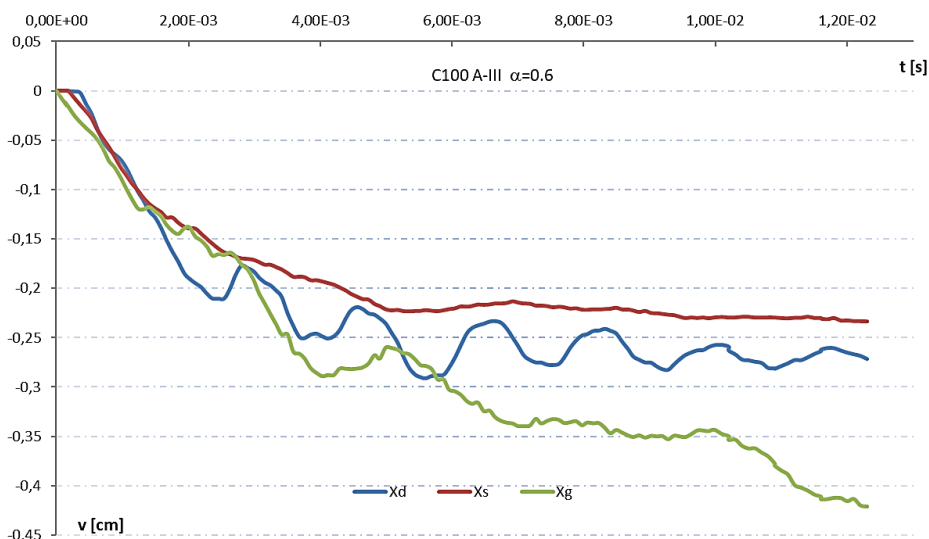


Fig. 4_{5b}. Change over time of vertical displacements of points in the central section for the load level $\alpha = 0.6$ — detail fig. 4_{5a} (with a reduced time interval of the analysis)

of deformation of the deep beam fig. 4_{5a}, fig. 4_{5b}, the symptoms of the oscillation of vertical displacement of point x_d around the point of balance could be observed. As an effect of the development of concrete cracked zones in two areas: diagonally from the shear zone to the upper layers of span section and in the lower span area, a loss of carrying capacity of the deep beam took place.

Fig. 5 shows the variability of vertical displacement over time of chosen points in the lower edge of the deep beam for various load levels $\alpha = P/P_0$. Within the range of plastic capacity of the construction, at load levels $\alpha = 0.1$ and $\alpha = 0.2$, (fig. 5₁) maximal deflection occurred in the span in point x_{18} , and the observed amplitude values of vertical displacements decreased monotonically towards the support. The same behaviour of the structure can be observed at load level $\alpha = 0.3$, (fig. 5₂), when scratching of concrete in proximity of the support occurred. At load level $\alpha = 0.4$, (fig. 5₃), a sudden increase in the displacement of point x_{10} can be observed, below the value of displacement of points in proximity of the central axis of the vertical symmetry. It is caused by the development of the area of scratched concrete in the proximity of that point — a propagation of the cracked area occurred in a vertical direction. Upon an additional increase of load to $\alpha = 0.5$, (fig. 5₄), a stabilisation of displacement of point x_{10} is observed. At the same time, a sudden increase in displacements can be observed in the following vertical points: x_{12} , x_{14} , x_{16} , x_{18} in relation to the manifestation of a new crack area in the central section and with the change of propagation of cracked area in shear zone from vertical to diagonal towards the central section. In fig. 5₅, which matches load level $\alpha = 0.6$,

further development of the cracked concrete area is visible. Concrete crack area in the lower part of the span section propagates upwards, which results in further increase of vertical displacements of point x_{18} . However, a much higher increase in vertical displacement was observed in point x_{12} , which is located in shear zone and adjacent to point x_{10} , which was cracked first. As a result, an unimpeded increase in vertical displacements occurred successively in points x_{16} , x_{18} , x_{14} — it is a clear sign of the depletion of carrying capacity and destruction of the analysed deep beam.

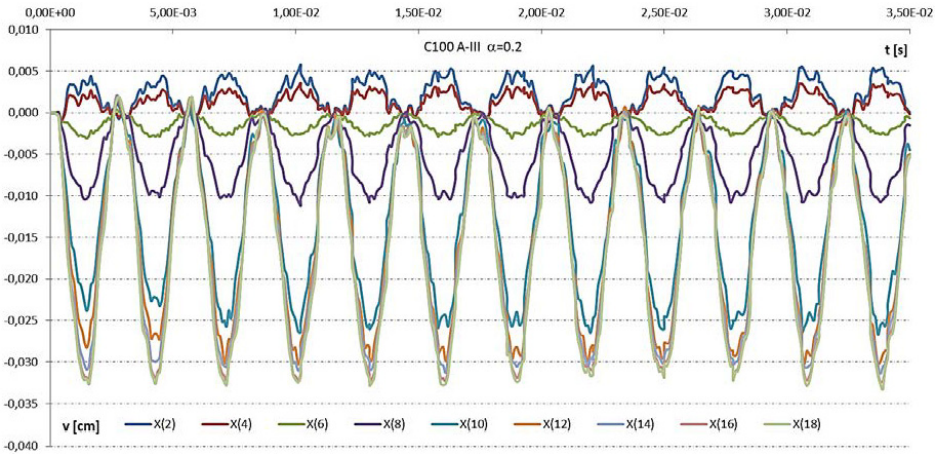


Fig. 5₁. Change over time of vertical displacements of points in the lower edge of the deep beam for load level $\alpha = 0.2$

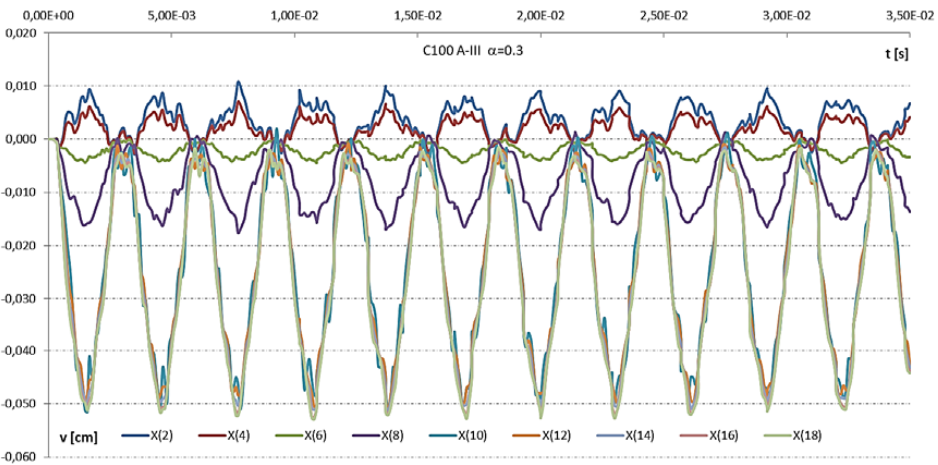


Fig. 5₂. Change over time of vertical displacements of points in the lower edge of the deep beam for load level $\alpha = 0.3$

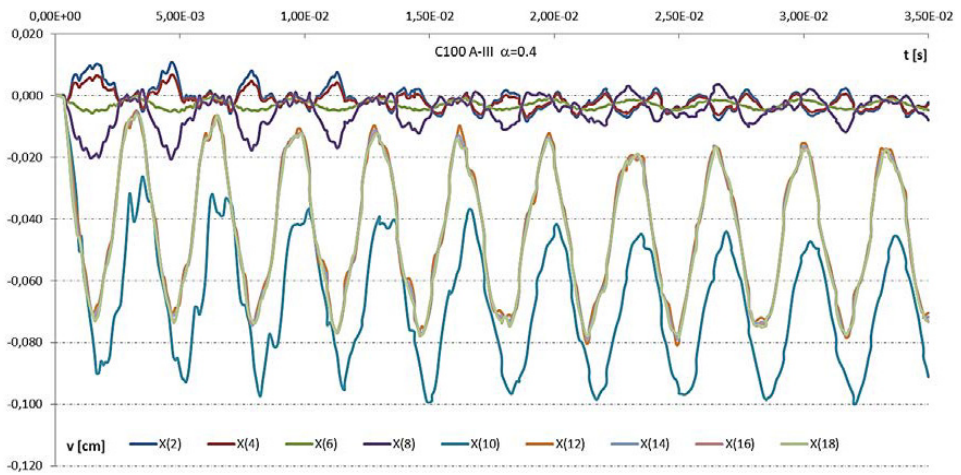


Fig. 5₃. Change over time of vertical displacements of points in the lower edge of the deep beam for load level $\alpha = 0.4$

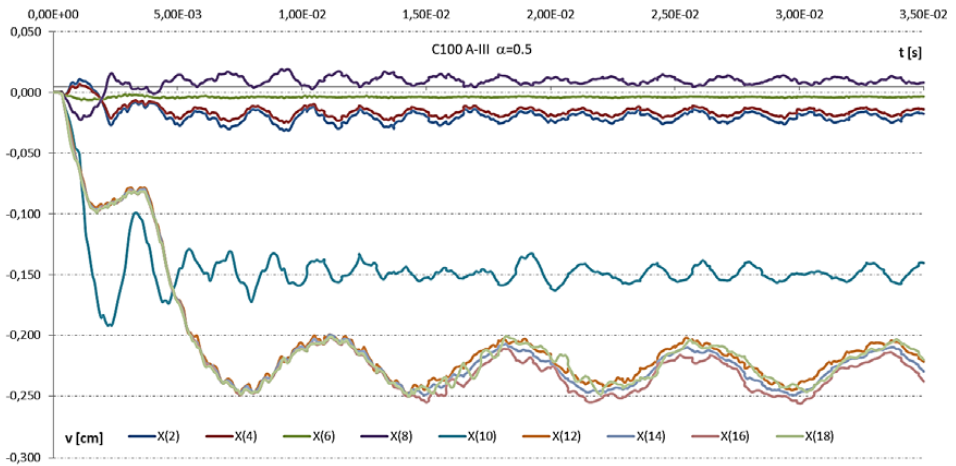


Fig. 5₄. Change over time of vertical displacements of points in the lower edge of the deep beam for load level $\alpha = 0.5$

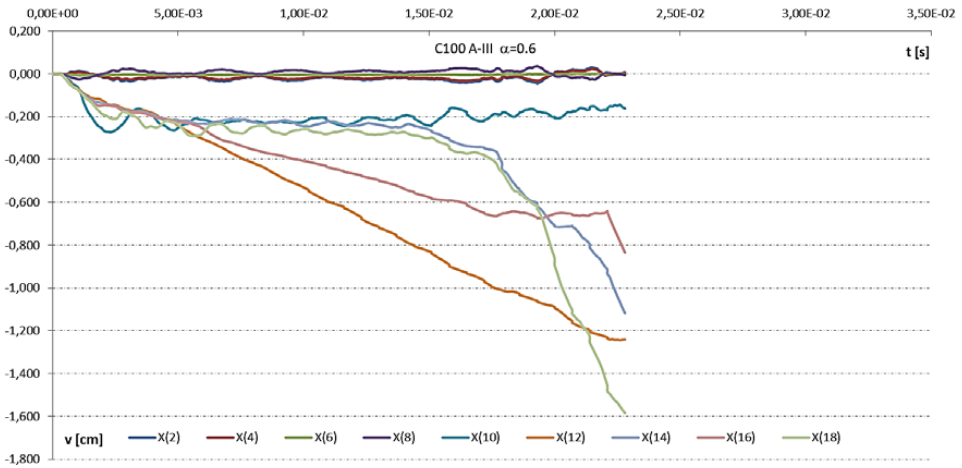


Fig. 5₅. Change over time of vertical displacements of points in the lower edge of the deep beam for load level $\alpha = 0.6$

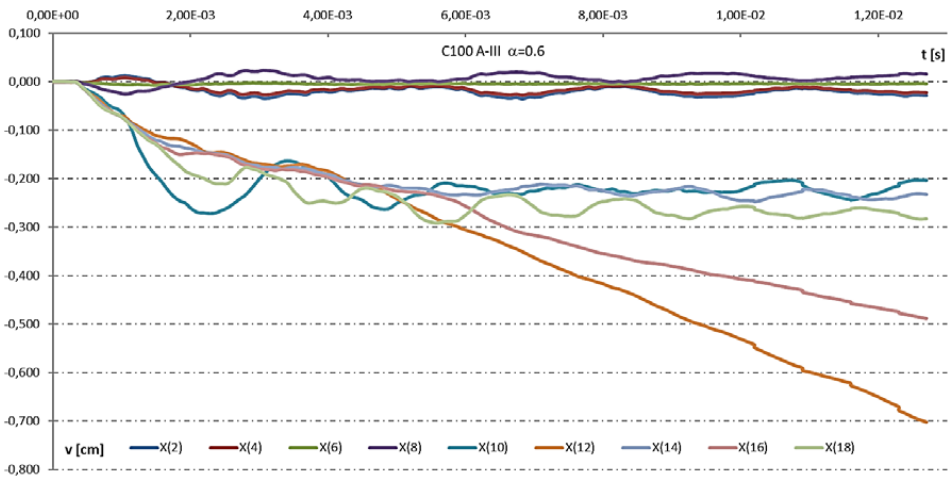


Fig. 5_{5a}. Change over time of vertical displacements of points in the lower edge of the deep beam for load level $\alpha = 0.6$ — detail fig. 5₅ (with a reduced time interval of the analysis)

Fig. 6 shows the variability of vertical displacement over time of chosen points in the upper edge of the deep beam for various load levels $\alpha = P/P_0$. At load levels $\alpha = 0.1$, $\alpha = 0.2$, (fig. 6₁), $\alpha = 0.3$, (fig. 6₂) and $\alpha = 0.4$, (fig. 6₃), the maximal deflection occurred in the span in point x_{306} , and observed amplitude values of vertical displacements decrease monotonically towards the support. The same behaviour of the structure can be observed at load level $\alpha = 0.5$, (fig. 6₄) — however, because of advanced processes of concrete cracking, a differentiation of the dynamic

equilibrium level, i.e. permanent displacements of each point on the upper edge, is visible. As a result, the vertical displacements of each point display vibrating motion, but only around varied equilibrium levels. In fig. 6₅, which matches load level $\alpha = 0.6$, further development of the concrete cracked area is visible — an unimpeded increase in vertical displacements adjacent to the central section commences successively in points x_{306} and x_{302} , which signals depletion of carrying capacity and destruction of the analysed deep beam.

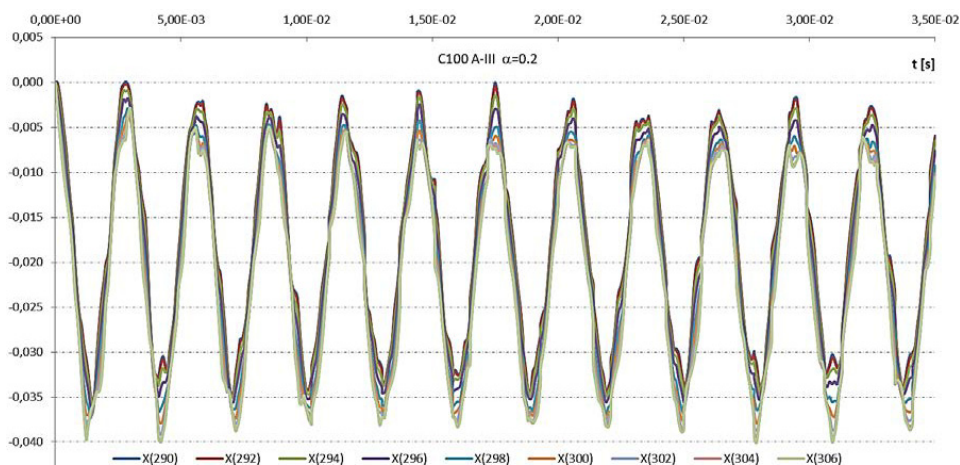


Fig. 6₁. Change over time of vertical displacements of points in the upper edge of the deep beam for load level $\alpha = 0.2$

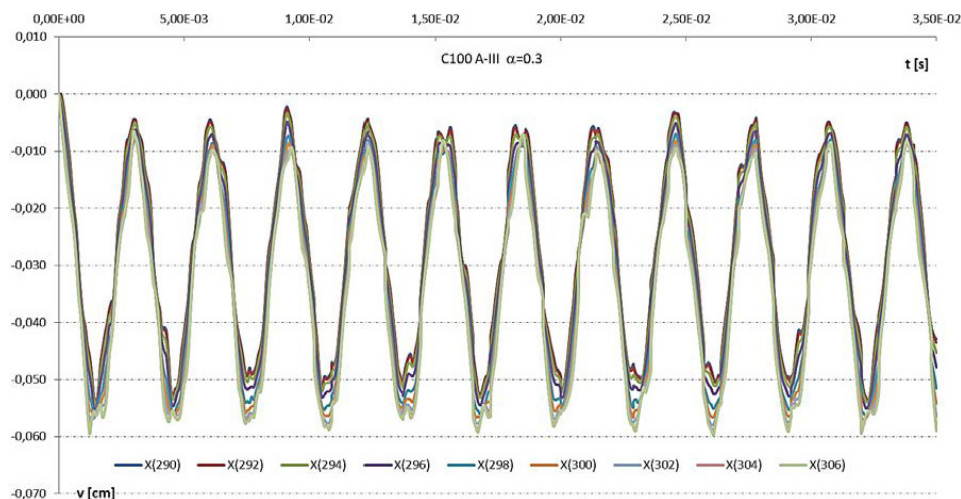


Fig. 6₂. Change over time of vertical displacements of points in the upper edge of the deep beam for load level $\alpha = 0.3$

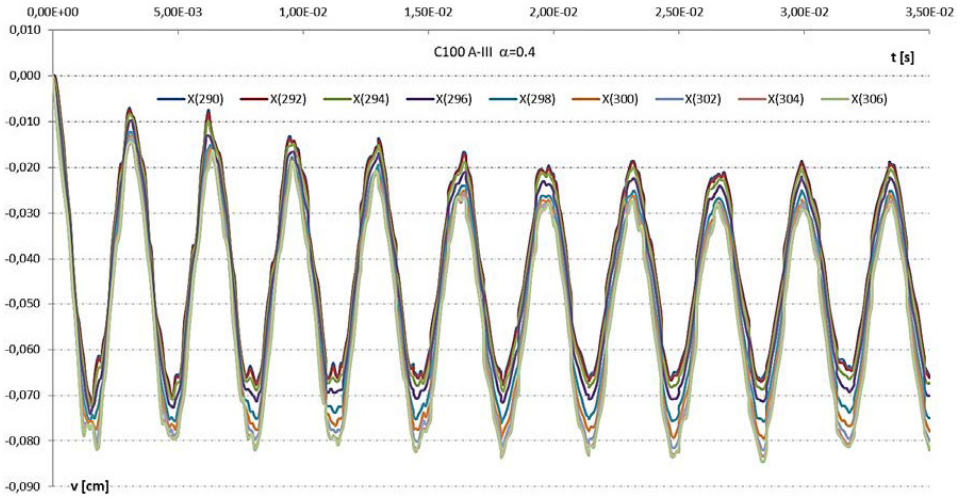


Fig. 63. Change over time of vertical displacements of points in the upper edge of the deep beam for load level $\alpha = 0.4$

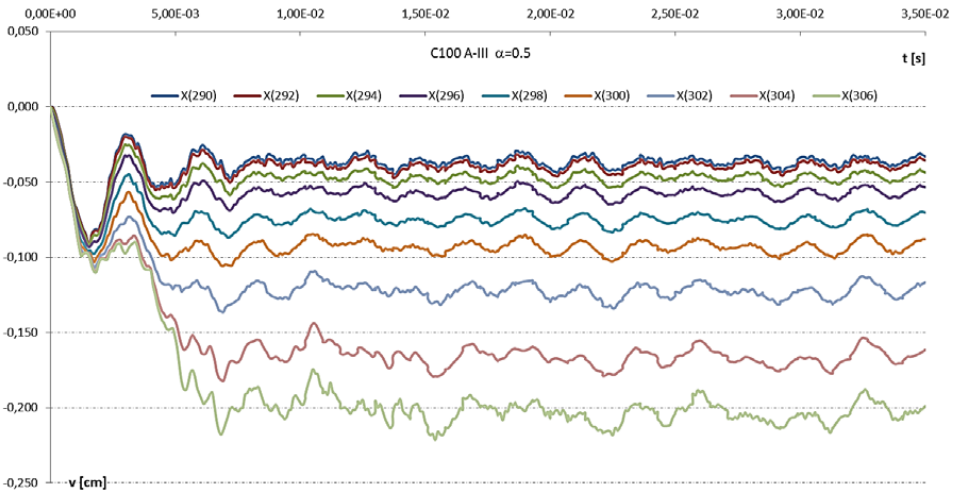


Fig. 64. Change over time of vertical displacements of points in the upper edge of the deep beam for load level $\alpha = 0.5$

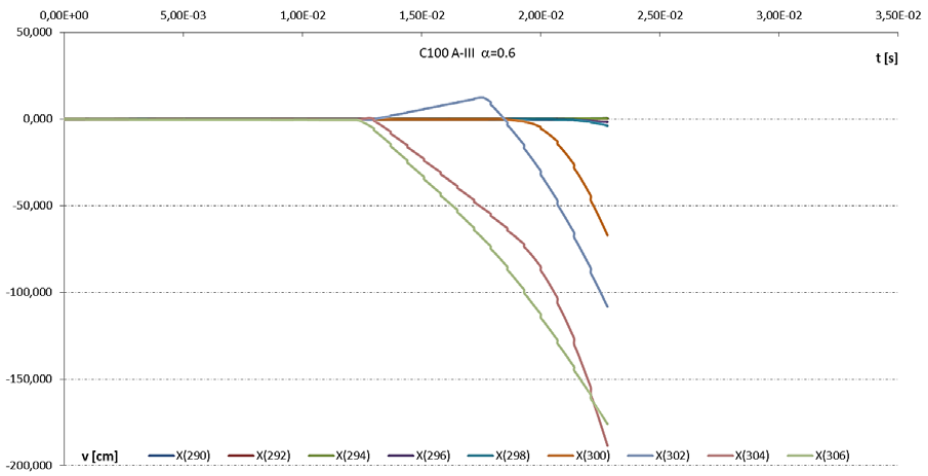


Fig. 6₅. Change over time of vertical displacements of points in the upper edge of the deep beam for load level $\alpha = 0.6$

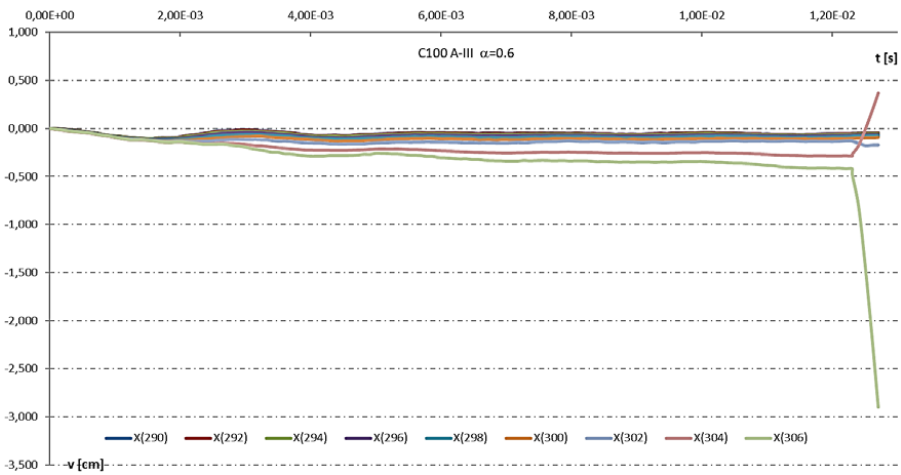


Fig. 6_{5a}. Change over time of vertical displacements of points in the upper edge of the deep beam for load level $\alpha = 0.6$ — detail fig. 6₅ (with a reduced time interval of the analysis)

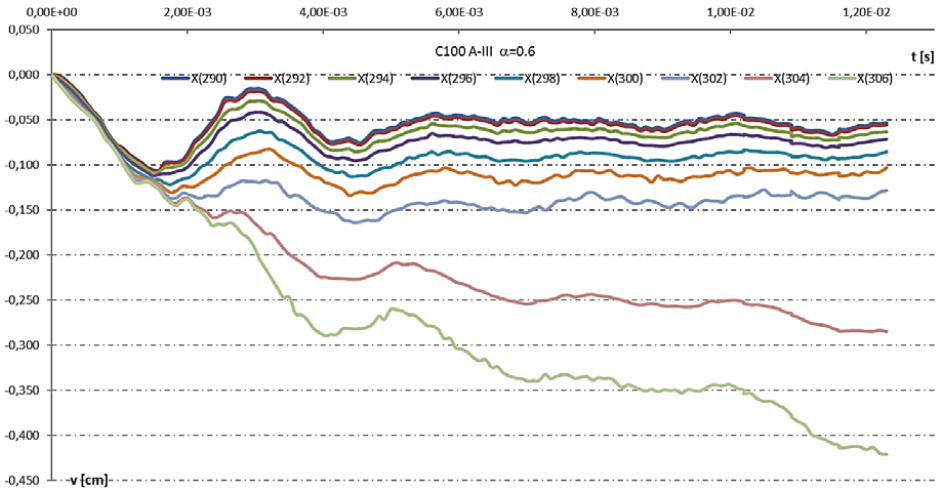


Fig. 6_{5b}. Change over time of vertical displacements of points in the upper edge of the deep beam for load level $\alpha = 0.6$ — detail fig. 6_{5a} (with a reduced time interval of the analysis)

2.2. Reinforced-concrete deep beam reinforced with ordinary steel (A-H)

Fig. 7 shows the variability of vertical displacement over time of chosen points in the central section for various load levels $\alpha = P/P_0$. For load level $\alpha = 0.3$, fig. 7₁, and fig. 7₂, in the elastic range and with a minor level of plastic processes in concrete, the results indicate the relation known from elastic solutions between vertical displacements: $v(x_g) > v(x_s) > v(x_d)$, the same as for C100 concrete deep beam and reinforced with A-III steel. As the load increases to level $\alpha = 0.4$, fig. 7₃, a significant increase of vertical displacements of the lower point x_d are observed. In spite of cracking the concrete in lower layers in the shear zone (similarly to the case of the deep beam reinforced with A-III steel), modification of interrelations between the change over time of each vertical displacement, i.e. contrary to the results with the deep beam reinforced with A-III steel, did not occur. With a further increase in the application of load to level $\alpha = 0.5$, fig. 7₄, a propagation of cracked areas in the shear zone took place, however in a manner different from the case of the deep beam reinforced with A-III steel, i.e. only in a vertical direction. At the same time no development of cracks in the span section was identified, unlike in the deep beam reinforced with A-III steel. This caused a modification of the interrelations between the change over time of each vertical displacement, different from the one in the deep beam reinforced with A-III steel (for the same load level): $v(x_g) > v(x_s) \cong v(x_d)$, which applies at intervals of reaching maximum amplitude of displacements. At load level $\alpha = 0.6$, fig. 7₅, a further development of stable plastic processes (different from the case of the deep beam reinforced with A-III steel (for the same

load level) can be observed, which was manifested by stabilised vibrating motion around permanent displacements of observed points. Only at this level of loading (the same as in the deep beam reinforced with *A-III* steel at load level $\alpha = 0.5$) the propagation of cracked areas took place in the shear zone diagonally towards the centre of the span and a sudden propagation in the span area, which caused another modification of interrelation between the change over time of each vertical displacement, different than in the deep beam reinforced with *A-III* steel at load level $\alpha = 0.5$): $v(x_d) > v(x_s) > v(x_g)$, which applies at intervals of reaching maximum amplitude of displacements. Unlike the case of the deep beam reinforced with *A-III* steel, at load level $\alpha = 0.7$, fig. 7₆, a lack of stabilisation of plastic processes can be observed, which manifested itself at lower levels of load stabilised by vibrating motion around permanent displacements of observed points. As an effect of the development of concrete cracked zones in two areas: initially diagonally from the shear zone to the span section and mostly in the central section, a loss of carrying capacity of the deep beam took place.

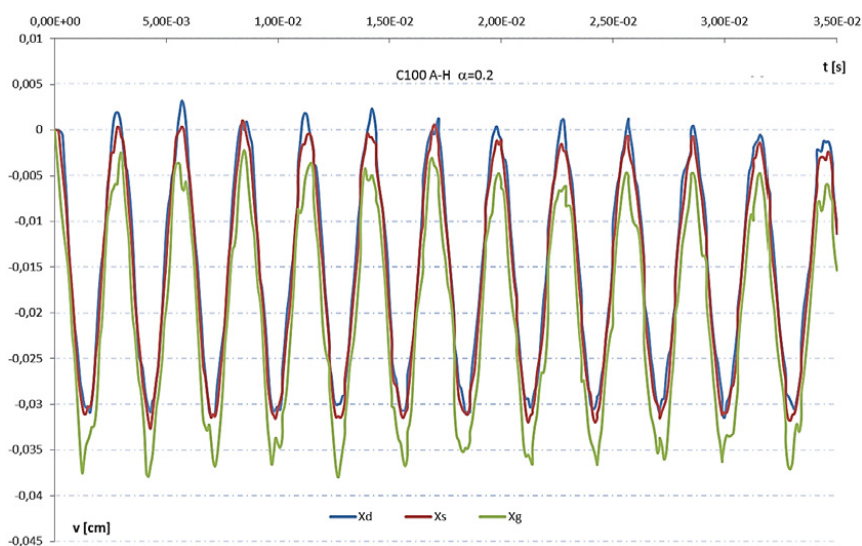


Fig. 7.1. Change over time of vertical displacements of points in the central section for load level $\alpha = 0.2$

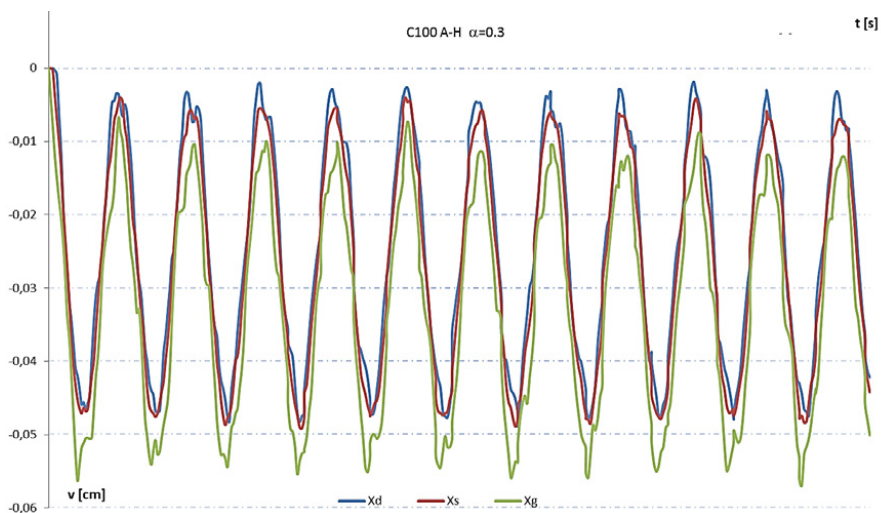


Fig. 7₂. Change over time of vertical displacements of points in the central section for load level $\alpha = 0.3$

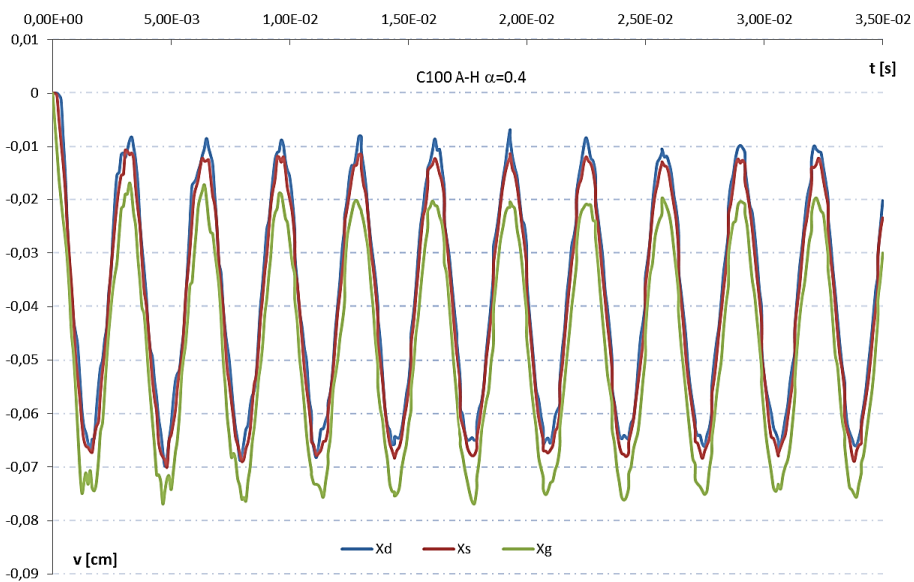


Fig. 7₃. Change over time of vertical displacements of points in the central section for load level $\alpha = 0.4$

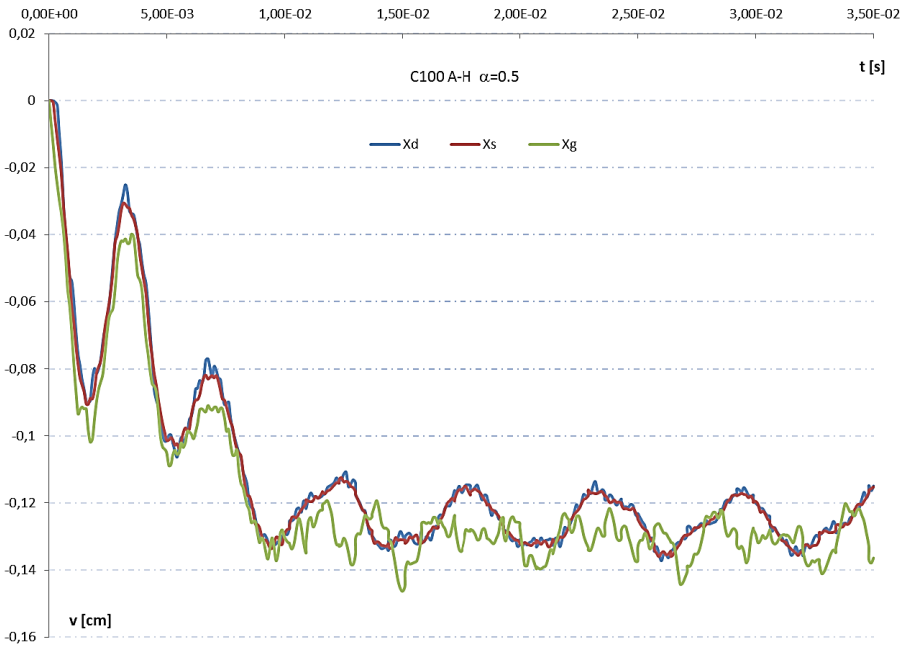


Fig. 7₄. Change over time of vertical displacements of points in the central section for load level $\alpha = 0.5$

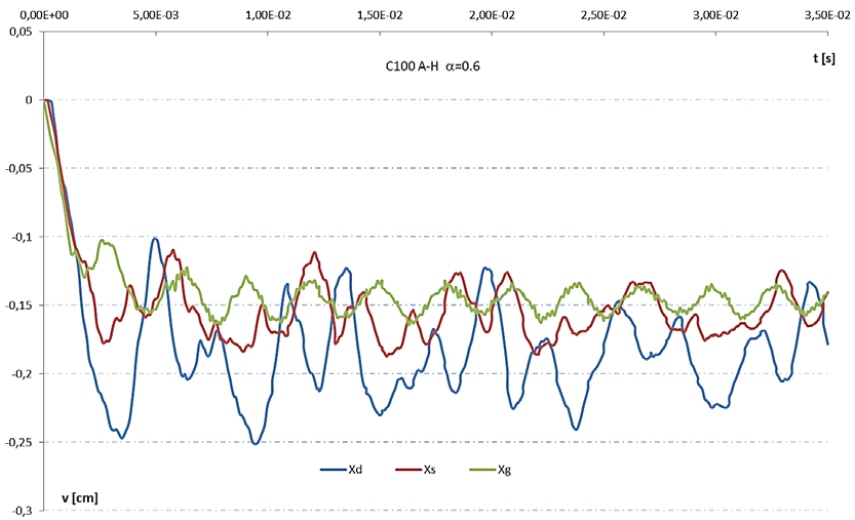


Fig. 7₅. Change over time of vertical displacements of points in the central section for load level $\alpha = 0.6$

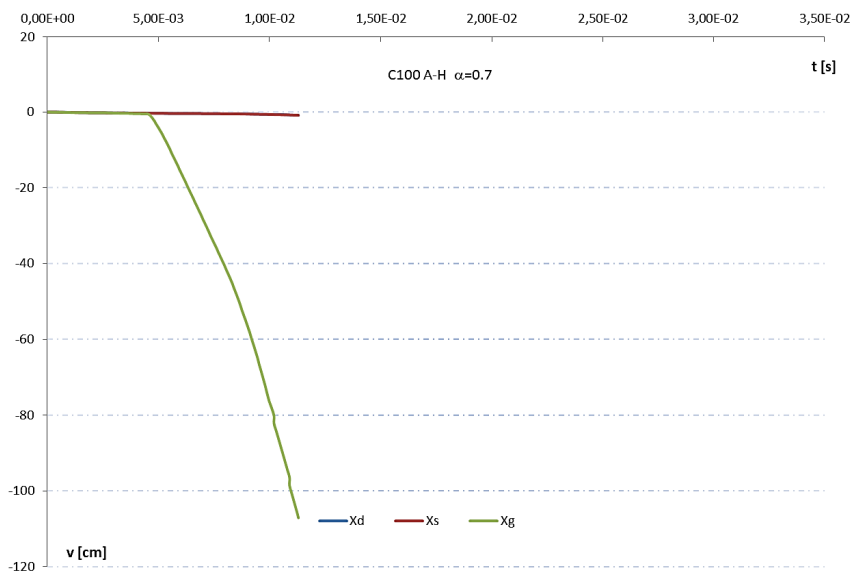


Fig. 7₆. Change over time of vertical displacements of points in the central section for load level $\alpha = 0.7$



Fig. 7_{6a}. Change over time of vertical displacements of points in the central section for load level $\alpha = 0.7$ — detail fig. 7₆ (with a reduced time interval of the analysis)

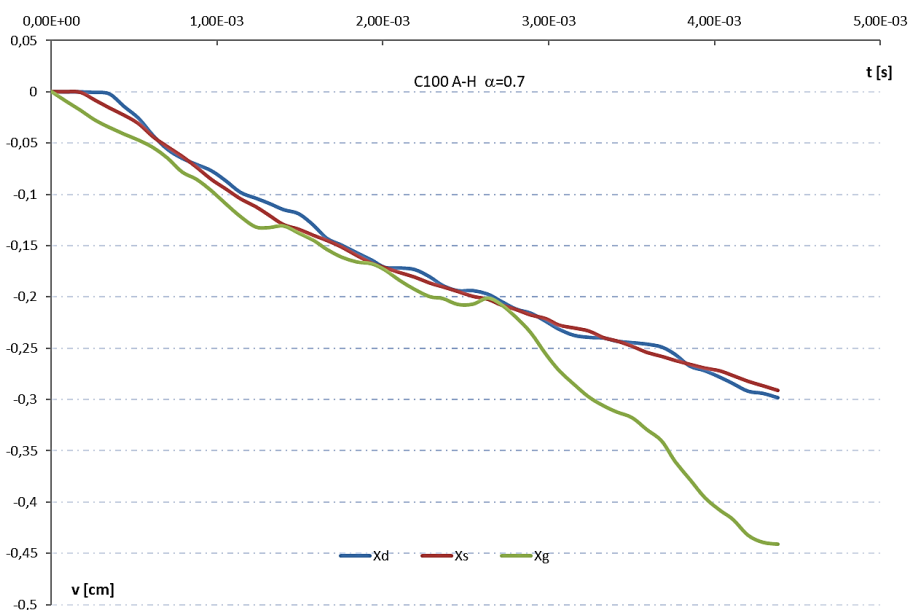


Fig. 7_{6b}. Change over time of vertical displacements of points in the central section for the load level $\alpha = 0.7$ — detail fig. 7_{6a} (with a reduced time interval of the analysis)

Fig. 8 shows the variability of vertical displacement over time of chosen points in the lower edge of the deep beam for various load levels $\alpha = P/P_0$. In the range of elastic capacity of the construction, at load levels $\alpha = 0.1$ and $\alpha = 0.2$, (fig. 8₁) maximal deflection occurred, just like in the deep beam reinforced with A-III steel, in the span in point x_{18} , and observed amplitude values of vertical displacements decrease monotonically towards the support. Also, at load level $\alpha = 0.3$, (fig. 8₂), the same behaviour of the structure can be observed, when scratching of concrete in proximity to the support occurred. At load level $\alpha = 0.4$, (fig. 8₃), just like in the deep beam reinforced with A-III steel, a sudden increase in displacement of point x_{10} occurs, exceeding the values of displacements of points adjacent to the central axis of the vertical symmetry. It is caused by the development of the area of cracked concrete in proximity to that point — a propagation of the scratched area occurred in a vertical direction. Upon the additional increase of load to $\alpha = 0.5$, (fig. 8₄), a stabilisation of displacement of point x_{10} is observed. At the same time, an increase in displacements can be observed in the following vertical points: x_{12} , x_{14} , x_{16} , x_{18} adjacent to the central section — this increase, however, is significantly smaller than in the case of the deep beam reinforced with A-III steel. It is caused by the difference in the development of concrete cracked areas. Currently, just as in the deep beam reinforced with A-III steel, a change occurred in the direction of propagation of the cracked area in the shear zone from vertical to diagonal towards

the central section, however, unlike in the deep beam reinforced with *A-III* steel, concrete cracking in lower layers of the central section did not occur. Only at load level $\alpha = 0.6$, fig. 8₅, a sudden increase was observed in vertical displacements, however, only from point x_{18} in the central section because of the manifestation of a new cracked area in the central section (vertical cracks) and its sudden development in a vertical direction. At the same time, a further increase in displacements can be observed in point x_{10} . Observed displacement changes of the chosen points indicate an obvious change in the mechanism of cracking and effort of the deep beam caused by the change of reinforcing steel from *A-III* to *A-H*. In turn, in fig. 8₆, which matches load level $\alpha = 0.7$, further development of the cracked concrete area is visible. The concrete cracked area in the lower part of the span section propagates upwards, which results in a further increase of vertical displacements of points adjacent to the central section. As a result, an unimpeded increase in vertical displacements occurred successively in points x_{12} , x_{14} , x_{16} and x_{18} . It is an obvious sign of the depletion of carrying capacity and destruction of the analysed deep beam, however, at a different, higher load than in the deep beam reinforced with *A-III* steel.

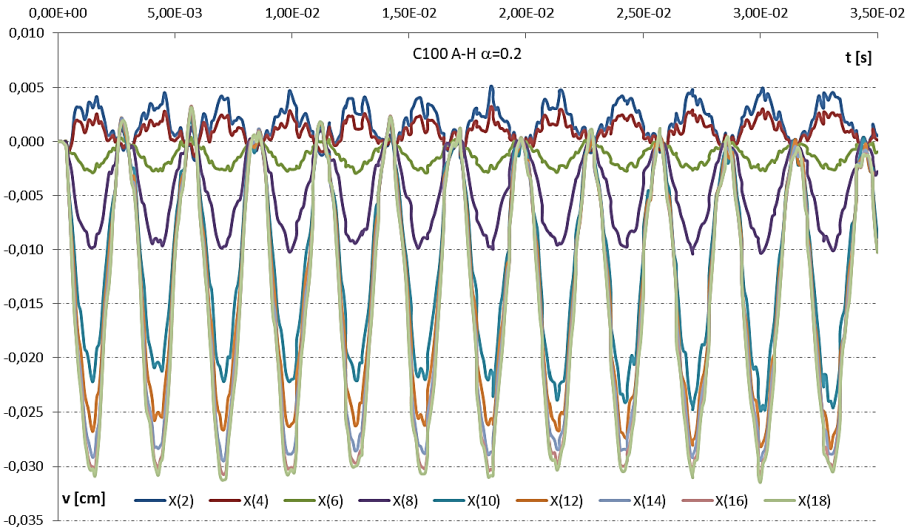


Fig. 8₁. Change over time of vertical displacements of points in the lower edge of the deep beam for load level $\alpha = 0.2$

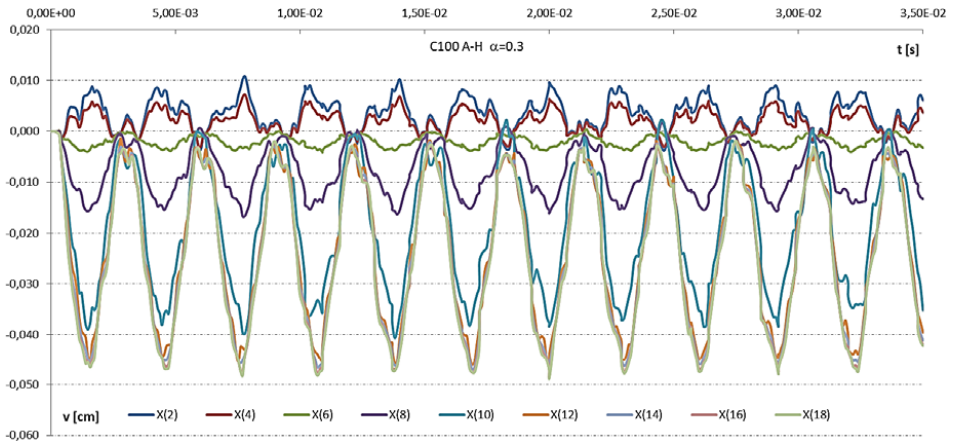


Fig. 8₂. Change over time of vertical displacements of points in the lower edge of the deep beam for load level $\alpha = 0.3$

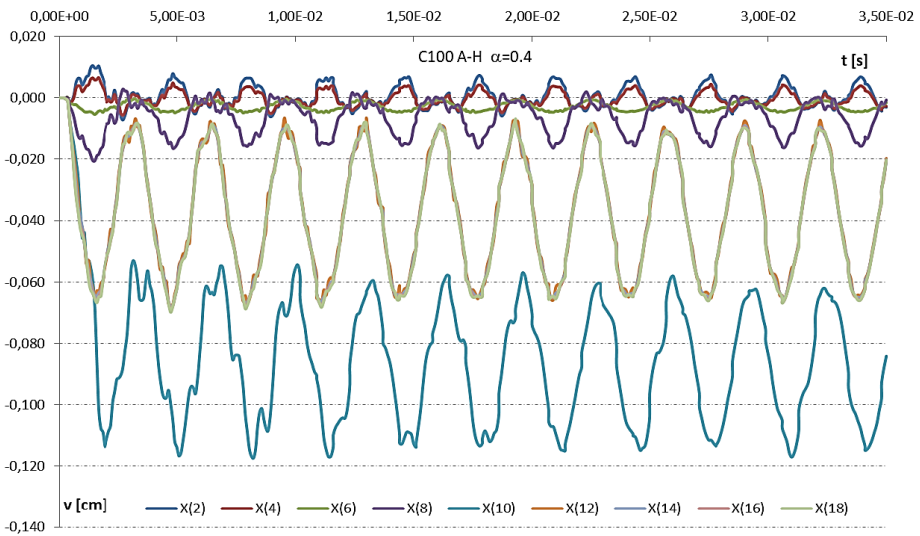


Fig. 8₃. Change over time of vertical displacements of points in the lower edge of the deep beam for load level $\alpha = 0.4$

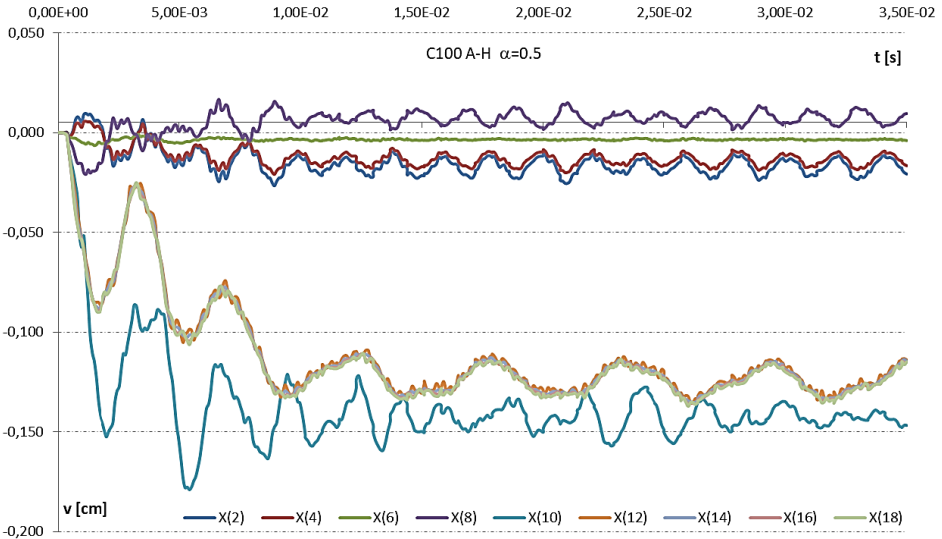


Fig. 8₄. Change over time of vertical displacements of points in the lower edge of the deep beam for load level $\alpha = 0.5$

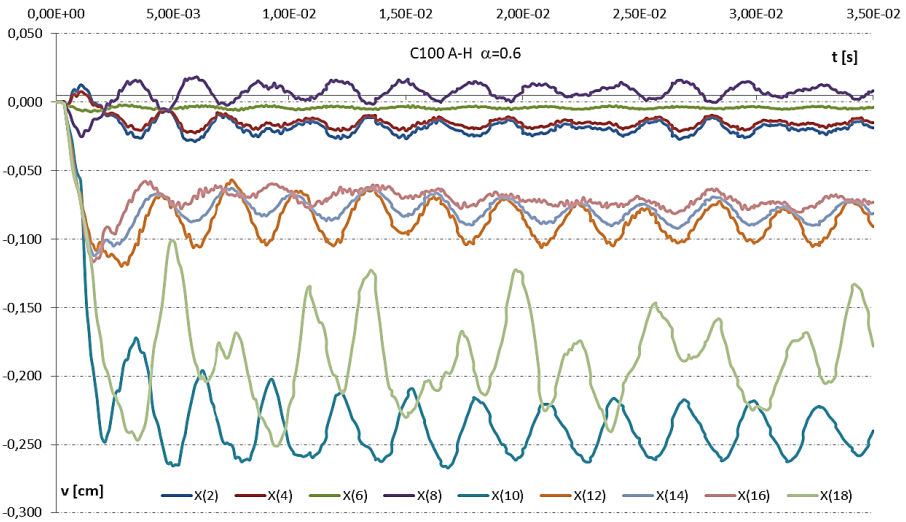


Fig. 8₅. Change over time of vertical displacements of points in the lower edge of the deep beam for load level $\alpha = 0.6$

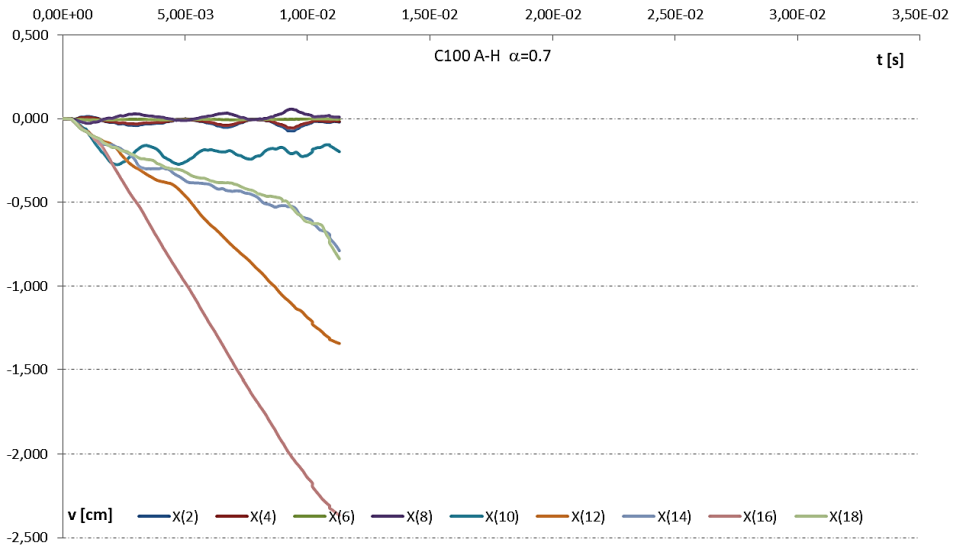


Fig. 8₆. Change over time of vertical displacements of points in the lower edge of the deep beam for load level $\alpha = 0.7$

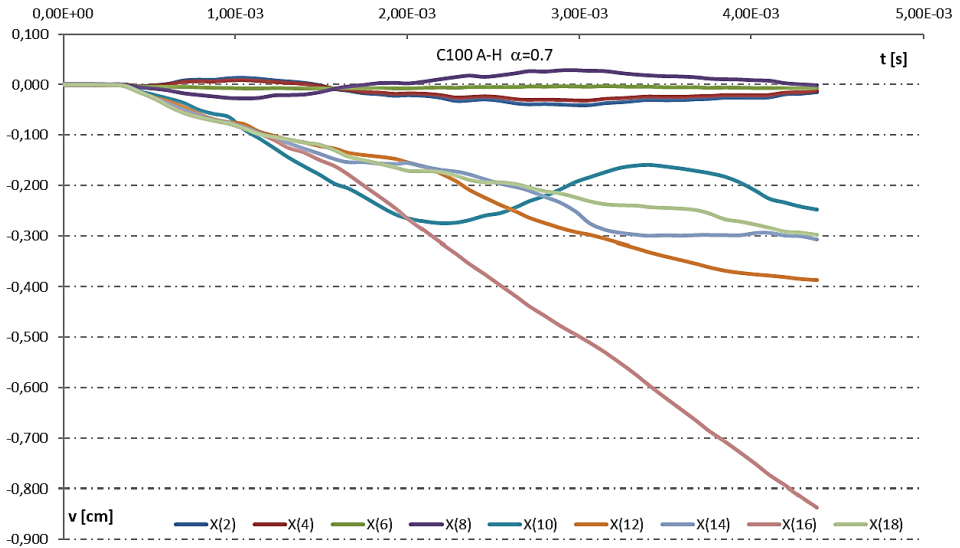


Fig. 8_{6a}. Change over time of vertical displacements of points in the lower edge of the deep beam for load level $\alpha = 0.7$ — limited time interval in relation to results in fig. 8₆

Fig. 9 shows the variability of vertical displacement over time of chosen points in the upper edge of the deep beam for various load levels $\alpha = P/P_0$. At load levels $\alpha = 0.1$, $\alpha = 0.2$, (fig. 9₁), $\alpha = 0.3$, (fig. 9₂) and $\alpha = 0.4$, (fig. 9₃) maximal deflection occurred, just as in the deep beam reinforced with A-III steel, in the span in point x_{306} , and the observed amplitude values of vertical displacements decrease monotonically towards the support. The same behaviour of the structure can be observed at load level $\alpha = 0.5$, (fig. 9₄) — however, because of the advanced processes of concrete cracking, a differentiation of the dynamic equilibrium level i.e. permanent displacements of each point on the upper edge, is visible. As a result, the vertical displacements of each point display vibrating motion, but only around varied equilibrium levels. The same behaviour of the structure can be observed at load level $\alpha = 0.6$, (fig. 9₅) — however, at this load level in the deep beam reinforced with A-III steel, its destruction has already occurred. In fig. 9₆, which matches load level $\alpha = 0.7$, further development of the concrete cracked area is visible — unimpeded increase in vertical displacements adjacent to the central section commences successively in points x_{304} and x_{306} , which signals depletion of carrying capacity and destruction of the analysed deep beam.

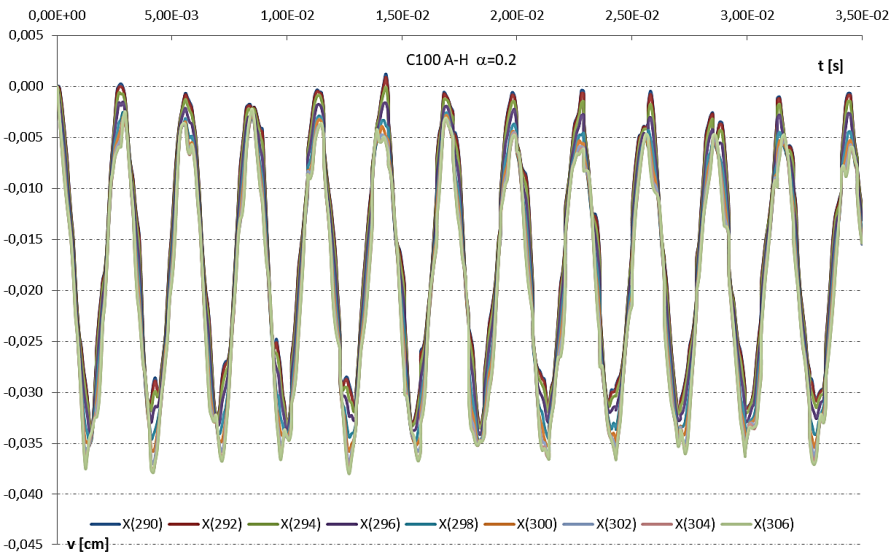


Fig. 9₁. Change over time of vertical displacements of points in the upper edge of the deep beam for load level $\alpha = 0.2$

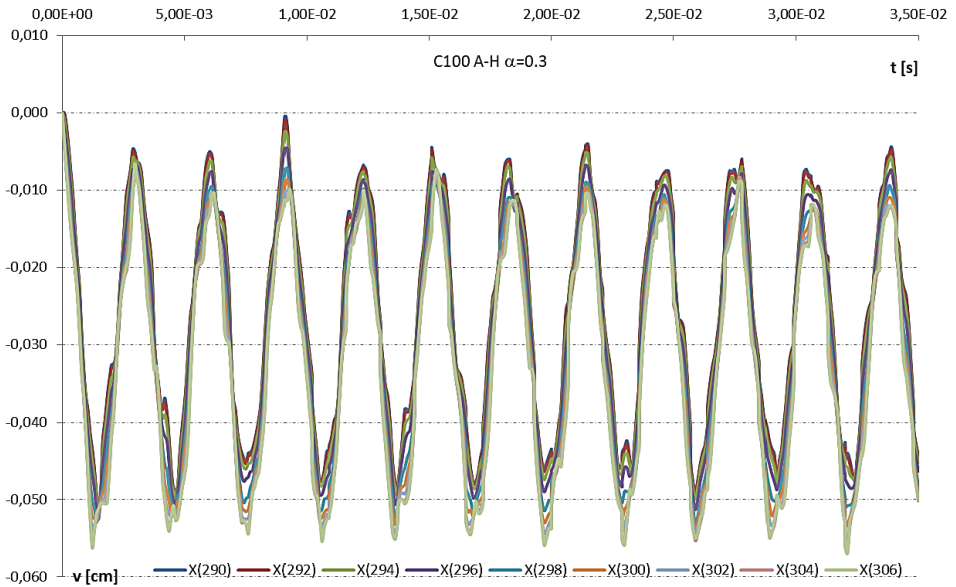


Fig. 9₂. Change over time of vertical displacements of points in the upper edge of the deep beam for load level $\alpha = 0.3$

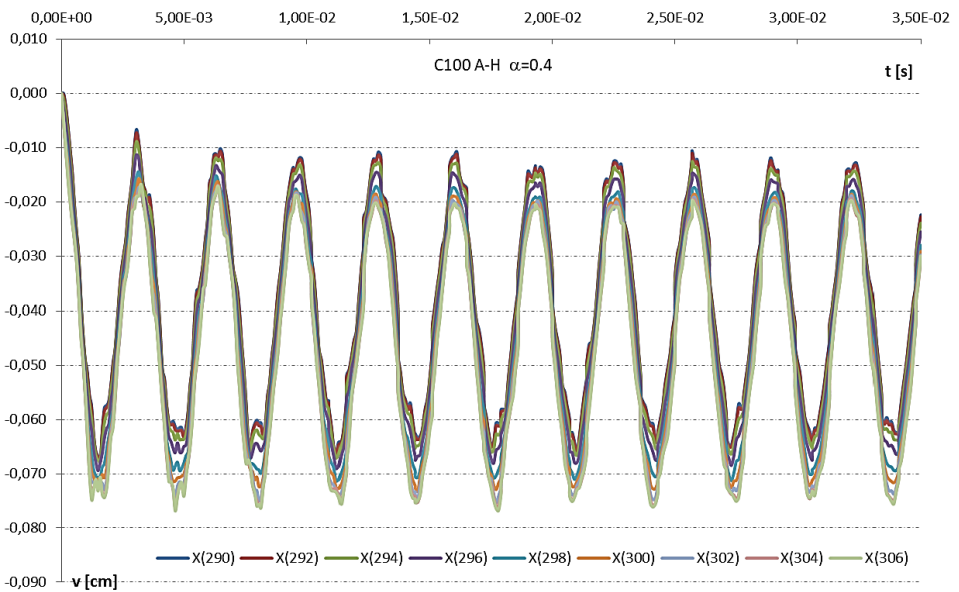


Fig. 9₃. Change over time of vertical displacements of points in the upper edge of the deep beam for load level $\alpha = 0.4$

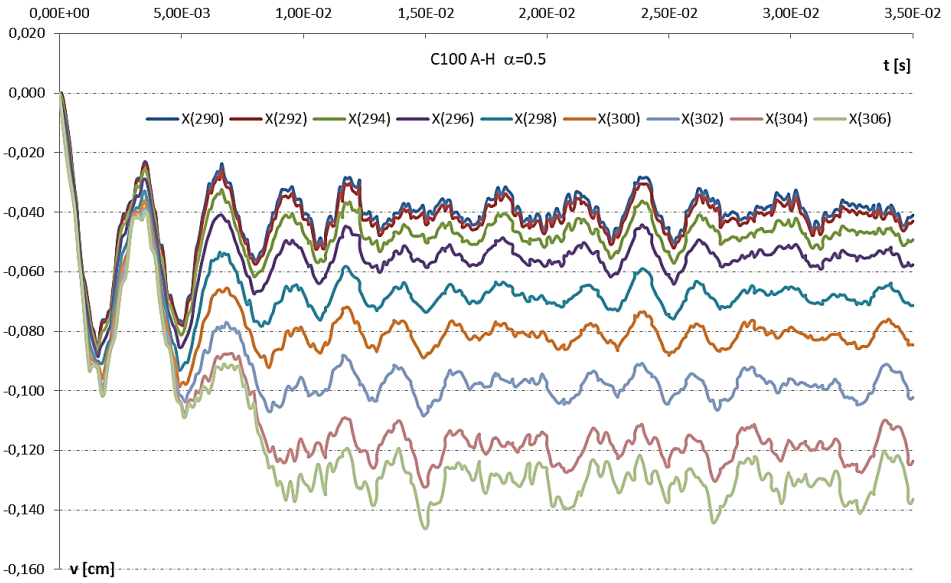


Fig. 9₄. Change over time of vertical displacements of points in the upper edge of the deep beam for load level $\alpha = 0.5$

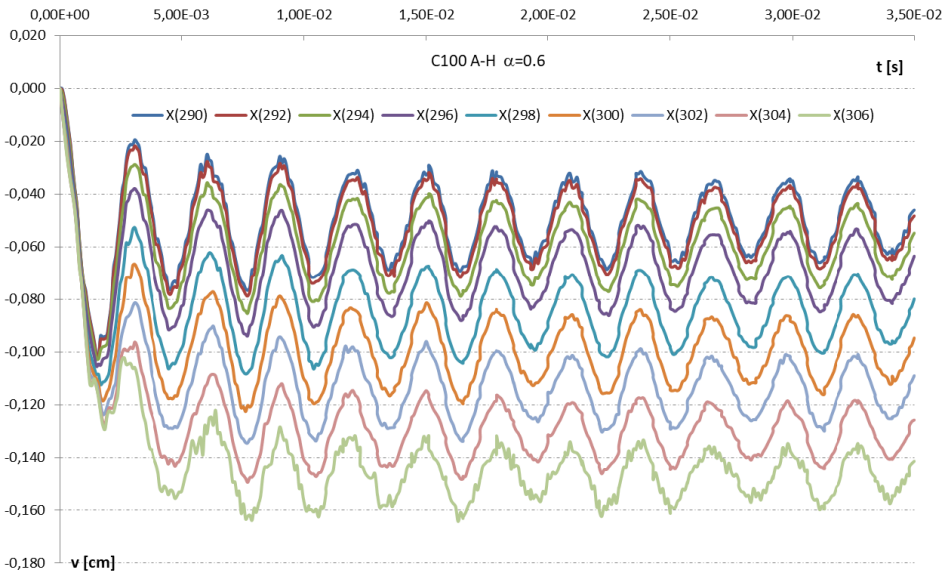


Fig. 9₅. Change over time of vertical displacements of points in the upper edge of the deep beam for load level $\alpha = 0.6$

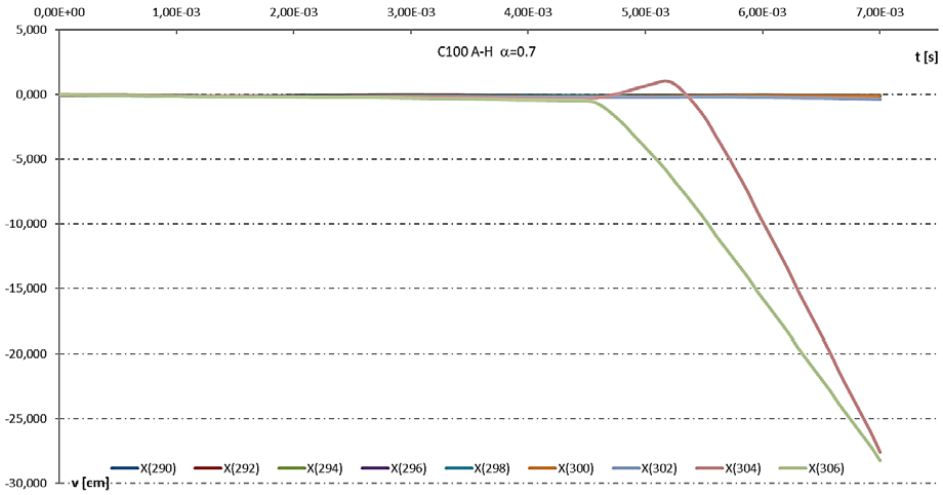


Fig. 9₆. Change over time of vertical displacements of points in the upper edge of the deep beam for load level $\alpha = 0.7$

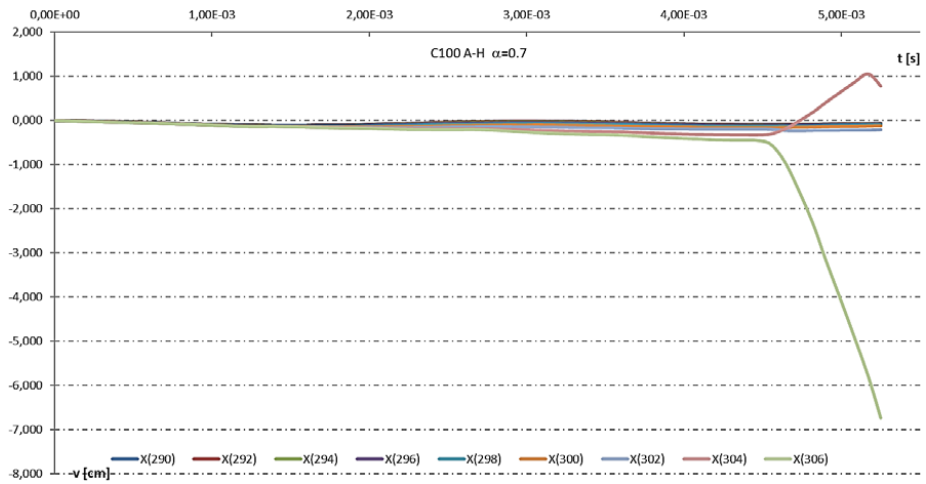


Fig. 9_{6a}. Change over time of vertical displacements of points in the upper edge of the deep beam for load level $\alpha = 0.7$ — detail fig. 9₆ (with a reduced time interval of the analysis)

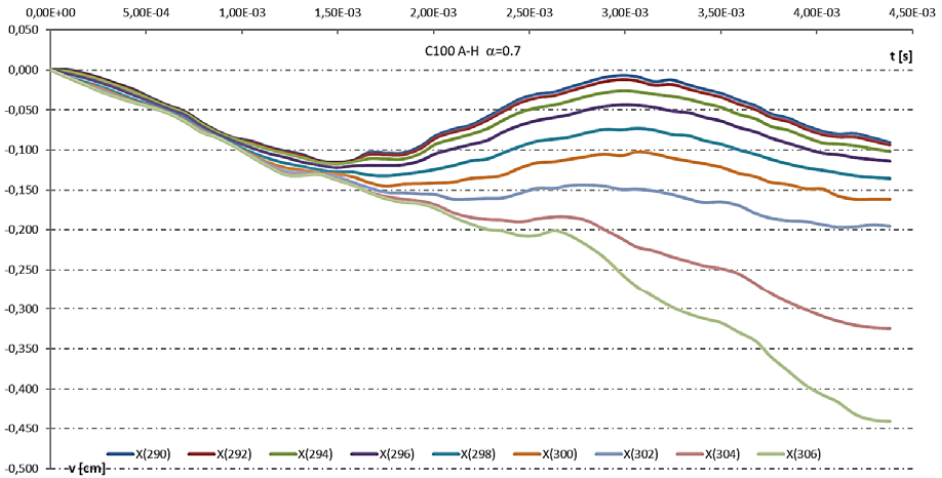


Fig. 9_{6b}. Change over time of vertical displacements of points in the upper edge of the deep beam for load level $\alpha = 0.7$ — detail fig. 9_{6a} (with a reduced time interval of the analysis)

3. Conclusion — summary of Part One

The work demonstrated the analysis of the displacement state of rectangular concrete deep beams made of very high strength concrete and steel of increased strength with dynamic load, including the physical nonlinearity of construction materials: concrete and reinforcing steel. A deformation analysis (displacement state) of the reinforced concrete deep beam was carried out in the function of a chosen parameter describing effort of the reinforced concrete structural element — steel strength. The subject of the analysis was a deep beam made of concrete of very high strength C100 grade. Analysis with consideration of such materials required the introduction of modifications in constitutive model parameters of structure materials. Deformation analysis of the deep beam was carried out on the basis of observation of changes in vertical displacement of chosen points on the lower and upper edges of the deep beam and in the central section. Within the framework of the analysis, it has been established that increasing the strength of steel may affect the mechanism of effort as well as destruction of a concrete deep beam in the form of a varied process of concentration and changes of cracked areas of the concrete matrix. The results of the analysis allowed for the demonstration of interrelations of the mechanism of achieving dynamic carrying capacity at the highest load level, at which no instabilities of displacement state occur. The results presented confirm the necessity of conducting studies of the influence of the constitutive model parameters of concrete of very high strength and steel of increased strength on the effort mechanism of reinforced concrete elements. Full analysis of the influence of changes in strength parameters of steel on deformation of the analysed deep beam requires conducting

additional analyses with changed parameters of high-strength concrete. The analysis will constitute a subject in further articles concerning deep beams made of C200 and C300 concrete. The results presented in this work point to the correctness of established assumptions and concrete deformation models and the effectiveness of the analysis method proposed in the work for problems of the numerical simulation of the dynamic behaviour of reinforced concrete deep beams.

The work was created as a result of research tasks carried out within the framework of the statutory research no 934, carried out in the Faculty of Civil Engineering and Geodesy of the Military University of Technology.

Received November 27, 2017. Revised February 5, 2018.

Paper translated into English and verified by company SKRIVANEK sp. z o.o., 22 Solec Street, 00-410 Warsaw, Poland.

REFERENCES

- [1] CICHORSKI W., STOLARSKI A., *Metoda analizy niesprężystego zachowania tarczy żelbetowej obciążonej dynamicznie*, Biuletyn WAT, 49, 10, 2000, 5-30.
- [2] STOLARSKI A., *Model dynamicznego odkształcania betonu*, Archiwum Inżynierii Lądowej, 37, 3-4, 1991, 405-447.
- [3] CICHORSKI W., STOLARSKI A., *Modelling of inelastic behaviour of reinforced concrete deep beam*, Journal of Achievements in Materials and Manufacturing Engineering, 44(1), 2016, 37-44.
- [4] STOLARSKI A., CICHORSKI W., *Influence of high strength of concrete and reinforced steel on dynamic behavior of reinforced concrete deep beams*, Proceedings of the 12th International Conference on Shock & Impact Loads on Structures, Singapore, 15-16 June 2017, 159-168.
- [5] KLEIBER M., *Metoda elementów skończonych w nieliniowej mechanice kontinuum*, PWN, Warszawa, 1985.
- [6] LEONHARDT F., WALTHER R., *Wandartige träger*, Report, Deutscher Ausschüb für Stahlbeton, 229, Berlin, Germany, 1966.
- [7] CICHORSKI W., STOLARSKI A., *Analiza stanu przemieszczenia niesprężystej tarczy żelbetowej obciążonej statycznie*, Biuletyn WAT, 50, 5, 2001, 5-20.
- [8] STOLARSKI A., CICHORSKI W., *Oszacowanie nośności tarczy żelbetowej z uwzględnieniem betonu bardzo wysokiej wytrzymałości*, Biuletyn WAT, 51, 2, 2002, 49-67.
- [9] CICHORSKI W., STOLARSKI A., *Analiza wytrzymałości tarczy żelbetowej z materiałów konstrukcyjnych bardzo wysokich wytrzymałości*, Biuletyn WAT, 65, 4, 2016, 143-165.
- [10] WINNICKI A., PEARCE C.J., BIĆCANIĆ N., *Viscoplastic Hoffman consistency model for concrete*, Comput. & Struct., 79, 2001, 7-19.
- [11] MARZEC I., TEJCHMAN J., WINNICKI A., *Computational simulations of concrete behaviour under dynamic conditions using elasto-visco-plastic model with non-local softening*, Computers & Concrete, 2015, 15 (4), 515-545.

W. CICHORSKI

Analiza dynamicznego przemieszczenia tarcz żelbetowych z betonu wysokiej wytrzymałości

Część I: Analiza dynamicznego przemieszczenia tarczy żelbetowej z betonu wysokiej wytrzymałości klasy C100

Streszczenie. Prezentowana praca jest trzyczęściowym zbiorem opracowań zawierających analizę porównawczą stanu przemieszczenia prostokątnych tarcz żelbetowych wykonanych z betonu różnych klas bardzo wysokiej wytrzymałości, obciążonych dynamicznie. Analiza została przeprowadzona na podstawie metody zaprezentowanej w pracy [1], umożliwiającej uwzględnienie fizycznych nieliniowości materiałów konstrukcyjnych: betonu i stali zbrojeniowej. Każda część pracy zawiera wyniki rozwiązań numerycznych stanu przemieszczenia tarcz oddzielnie dla klasy wytrzymałości betonu C100, klasy C200 i klasy C300, w każdym przypadku zbrojonej stalą zwykłą i stalą o podwyższonej wytrzymałości. Analiza porównawcza przeprowadzona jest w części drugiej i części trzeciej, w których odpowiednio porównywano wyniki uzyskane w tych częściach z wynikami otrzymanymi w częściach poprzednich. Analiza obejmuje wzajemne relacje mechanizmu osiągnięcia nośności dynamicznej. Wyniki opisujące zmienność przemieszczeń w czasie wskazują na charakterystyczne cechy wyężenia tarczy i umożliwiają wnioskowanie o osiągnięciu stanu nośności dynamicznej. Generalnie w pracy potwierdzono poprawność przyjętych założeń i modeli odkształcenia betonu i stali oraz efektywność metody analizy proponowanej w pracy [1] w odniesieniu do problemów numerycznej symulacji zachowania tarcz żelbetowych pod obciążeniem dynamicznym.

W pierwszej części pracy przedstawiono główne założenia przyjęte w ramach prowadzonej analizy. Przedstawiono charakterystykę materiałów konstrukcyjnych: betonu i stali zbrojeniowej z uwzględnieniem zmodyfikowanej koncepcji modelowania dynamicznych własności betonu jako materiału o bardzo wysokiej wytrzymałości. Przeprowadzono analizę stanu przemieszczenia prostokątnych tarcz żelbetowych wykonanych z betonu bardzo wysokiej wytrzymałości klasy C100 pod obciążeniem dynamicznym dla dwu rodzajów stali zbrojeniowej — zwykłej i podwyższonej wytrzymałości.

Słowa kluczowe: mechanika konstrukcji, konstrukcje żelbetowe, tarcze, obciążenie dynamiczne, nieliniowość fizyczna

DOI: 10.5604/01.3001.0011.8056